Campylobacter jejuni impairs sodium transport and epithelial barrier function via cytokine release in human colon

This article has been corrected since Advance Online Publication and an erratum is also printed in this issue

R Bücker[1], SM Krug[1], V Moos[2], C Bojarski[2], MR Schweiger[3], M Kerick[3], A Fromm[1], S Janßen[2], M Fromm[1], NA Hering[4], B Siegmund[2], T Schneider[2], C Barmeyer[2] and JD Schulzke[1]

Campylobacter jejuni **is the most prevalent cause of foodborne bacterial enteritis worldwide. Patients present with diarrhea and immune responses lead to complications like arthritis and irritable bowel syndrome. Although studies exist in animal and cell models, we aimed at a functional and structural characterization of intestinal dysfunction and the involved regulatory mechanisms in human colon. First, in patients' colonic biopsies, sodium malabsorption was identified as an important diarrheal mechanism resulting from hampered epithelial ion transport via impaired epithelial sodium channel (ENaC) β- and γ-subunit. In addition, barrier dysfunction from disrupted epithelial tight junction proteins (claudin-1, -3, -4, -5, and -8), epithelial apoptosis, and appearance of lesions was detected, which cause leak-flux diarrhea and can perpetuate immune responses. Importantly, these effects in human biopsies either represent direct action of *Campylobacter jejuni* (ENaC impairment) or are caused by proinflammatory signaling (barrier dysfunction). This was revealed by regulator analysis from RNA-sequencing (cytometric bead array-checked) and confirmed in cell models, which identified interferon-γ, TNFα, IL-13, and IL-1β. Finally, bioinformatics' predictions yielded additional information on protective influences like vitamin D, which was confirmed in cell models. Thus, these are candidates for intervention strategies against *C. jejuni* infection and post-infectious sequelae, which result from the permissive barrier defect along the leaky gut.**

INTRODUCTION

Campylobacter jejuni (*C. jejuni*) are spiral-shaped, gram-negative bacteria, belonging to the group of epsilon-proteobacteria, including the genus *Helicobacter*, *Arcobacter*, and *Campylobacter* that can inhabit mucosal tissues of the gastrointestinal tract. The *C. jejuni* infection is currently the most common cause of foodborne bacterial gastroenteritis worldwide. The campylobacteriosis is characterized by diarrhea and intestinal inflammation, accompanied by abdominal cramps, nausea, chills, or fever. Sequelae of the campylobacteriosis are reactive arthritis, Guillain–Barré syndrome or irritable bowel syndrome (IBS). Histological observations of experimental *C. jejuni*-infected animals revealed acute inflammatory activity with focal mucosal lesions together with neutrophils infiltrating the crypt epithelium (cryptitis), described for the small intestine in mouse models[1] or for the colon of infected infant macaques.[2] The severity of mucosal lesions in the gastrointestinal tract of *C. jejuni*-infected NFκB-deficient mice could be assigned to the bacterial virulence factor cytolethal distending toxin (CDT).[3] CDT and other virulence factors were shown to be secreted via outer membrane vesicles (OMVs) and induce epithelial damage and cytokine release.[4,5] The *C. jejuni* diarrhea is categorized as inflammatory diarrhea, but a deeper characterization of underlying pathogenic processes in the epithelium leading to this diarrhea is lacking. Although some intestinal pathogens may have one central

[1]Institute of Clinical Physiology/Nutritional Medicine, Charité—Universitätsmedizin Berlin, Berlin, Germany. [2]Department of Gastroenterology, Infectious Diseases and Rheumatology, Charité—Universitätsmedizin Berlin, Berlin, Germany. [3]Laboratory of Functional Epigenomics, Functional Epigenomics, CCG, University Hospital of Cologne, Cologne, Germany and [4]Department of General, Visceral and Vascular Surgery, Charité—Universitätsmedizin Berlin, Berlin, Germany. Correspondence: JD Schulzke (joerg.schulzke@charite.de)

Received 9 December 2016; accepted 13 June 2017; published online 2 August 2017. doi:10.1038/mi.2017.66

pathomechanism, e.g., cholera toxin, usually more than one or even a potpourri of mechanisms including transport and barrier disturbance are observed. Clinical examinations of *C. jejuni*-infected humans revealed that the acute inflammatory response is a hallmark of the *C. jejuni* infection,[6,7] in which mucosal invasion is a main virulence characteristic of *C. jejuni*.[8] *C. jejuni* when invaded into the subepithelium can induce inflammation leading to leukocyte infiltration of crypts also in man.[8] Transmigration of *C. jejuni* through the intestinal epithelium occurs without immediate changes in barrier integrity, as indicated in several *in vitro* studies by stable transepithelial electrical resistance (TER) during *C. jejuni* invasion.[9] *C. jejuni* penetrates the tissue via the transcellular or the paracellular route.[10] Hours to days after *C. jejuni* invasion, impairment of epithelial barrier function[9,10] and changes in tight junction (TJ) protein expression were shown for occludin and claudin-1 in the human T84 colon carcinoma cell line or claudin-4 in canine SCBN intestinal epithelial cells.[11,12] In addition to the direct interaction of *C. jejuni* with intestinal epithelial cells, induction of cytokines, as e.g. IFNγ, were shown to have synergistic effects on barrier integrity and cytotoxicity,[13] but other Th1 cytokines like TNFα are also important regulators of TJ proteins and apoptosis.[14]

The question remains whether these pathologies described in animal and cell models are present also in the infected human mucosa and whether other mechanisms contribute to the *C. jejuni*-induced diarrhea. In the present study, we tested several pathomechanisms proposed for *C. jejuni* in the mucosa of patients suffering from campylobacteriosis and could directly identify different pathomechanisms leading to epithelial dysfunction and diarrhea by *C. jejuni* infection in human colonic samples.

RESULTS

Impaired epithelial Na^+ channel function in *C. jejuni*-infected human colon

A functional defect of epithelial ion transport and barrier function of colon mucosae from *C. jejuni*-infected patients was assessed in Ussing chamber experiments (Study design: **Supplementary Figure S1** online and **Supplementary Table S1**). For NaCl and water absorption in human colon, diverse carriers and channels are important. As Na^+ transport in the distal colon is substantially dependent on the activity of epithelial sodium channel (ENaC), we tested the biopsies for amiloride-sensitive electrogenic Na^+ transport (J_{Na}) in the Ussing chamber. During stimulation of the *C. jejuni*-infected human mucosa with 3 nM aldosterone the maximum transport capacity for Na^+ by ENaC was diminished in comparison to healthy control mucosa (**Figure 1a**). mRNA expression analysis from RNA-sequencing (RNA-Seq) revealed that the β- and γ-ENaC subunits were inhibited compared with controls (**Figure 1b**).

Unchanged epithelial anion secretion in *C. jejuni*-infected colon

Basal short-circuit current (I_{SC}) was not increased in *C. jejuni*-infected patients, and this held true also after correction for the respective epithelial-to-subepithelial resistance ratios (**Table 1**). Thus, when studied as a possible mechanism of diarrhea, *C. jejuni* did not trigger active anion secretion in this phase of the infection.

A recent study showed that *C. jejuni* can affect Cl^- secretion in T84 cells.[15] In our study, colon biopsies were tested in the Ussing chamber experiments after stimulation of electrogenic Cl^- secretion either with PGE_2 and theophylline (by cAMP-dependent activation) or with the cholinergic agonist carbachol (**Table 1**). We found that the maximum transport rate during

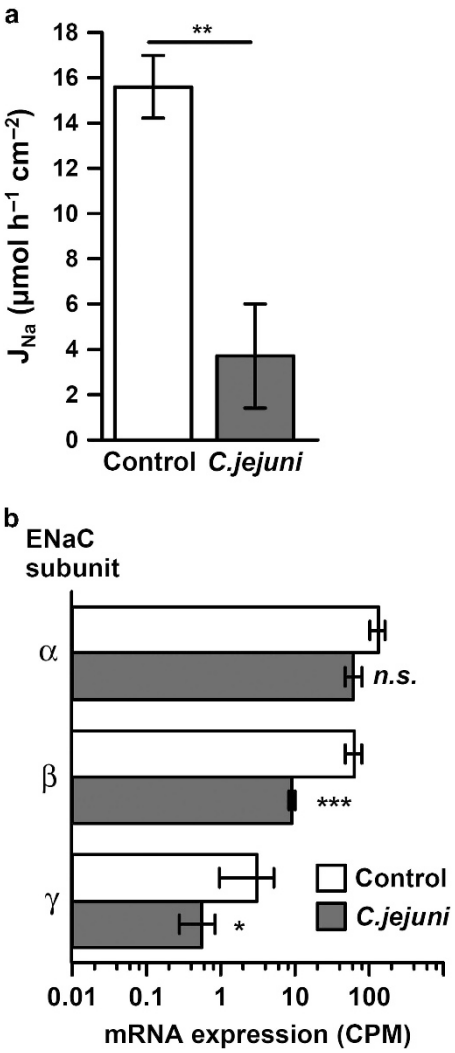

Figure 1 Electrogenic sodium transport in campylobacteriosis. (**a**) After mounting the human biopsy specimen into the Ussing chamber, aldosterone was added in a physiological concentration of 3×10^{-9} M to the mucosal and serosal compartments. Eight hours after addition of aldosterone, the epithelial sodium channel (ENaC) blocker amiloride (10^{-4} M) was added to the mucosal compartment and the resulting drop in I_{SC} was attributed to ENaC-dependent Na^+ flux (J_{Na}). Values were corrected for subepithelial resistance contributions in the Ussing chamber with R^t/R^{epi} ratios. $^*P<0.05$, Student's *t*-test, $n=4$. (**b**) mRNA expression of ENaC subunits. Differential gene expression analysis from RNA-Seq revealed mRNA expression of α-, β-, and γ-ENaC genes (SCNN1 to 3) from unstimulated biopsies. Normalized expression is illustrated as logarithmic function and reflects counts per million (CPM) as calculated by edgeR with $^*P<0.05$, $^{***}P<0.001$ vs. controls, *n.s.*, not significant, Fisher's exact test, $n=4$ *C. jejuni*-infected patients, $n=6$ controls. Data represent mean ± s.e.m.

Table 1 Active anion secretion in *C. jejuni*-infected mucosa and controls

	I_{SC} (μmol h^{-1} cm^{-2})		ΔI_{SC} (μmol h^{-1} cm^{-2})			*n*
	Basal	Basal	After PGE_2 + theophylline	After carbachol	After bumetanide	
	Uncorrected values	Corrected values with R^t/R^{epi}	Corrected values with R^t/R^{epi}			
Control	4.9 ± 1.2	6.4 ± 1.5	5.0 ± 1.0	9.3 ± 1.6	1.3 ± 0.3	6
C. jejuni	2.0 ± 0.2	3.2 ± 0.4	1.9 ± 0.6	3.7 ± 1.9	1.5 ± 0.4	6
P.	<0.05	n.s.	<0.05	<0.05	n.s.	

Abbreviations: n.s., not significant; PGE_2, prostaglandin E_2.
Data represent mean ± s.e.m. Student's t-test. Short-circuit currents (I_{SC}) were corrected for R^t/R^{epi}. Whenever the ratio of R^t over R^{epi} becomes significantly different, active transport parameters as I_{SC} need to be corrected, which follows the same principle like the correction of I_{SC} for the bath resistance (see also **Supplementary Methods**). In the *C. jejuni*-infected group, R^t/R^{epi} was 1.63 ± 0.10 and thus higher than in the control group with 1.29 ± 0.08 (n = 6 each, P < 0.05).

stimulation was diminished in infected patients. This could be due to the inhibition of Cl^- channels, like cystic fibrosis transmembrane activator (CFTR), as RNA-Seq analysis revealed that especially CFTR was downregulated in the mucosa of *C. jejuni* patients (logFold change −1.13, $P<0.05$). In addition, the anion exchanger DownRegulated-in-Adenoma (DRA, SLC26A3), an electroneutral transporter for Cl^- absorption, showed a reduced mRNA expression level (logFold change −1.33, $P<0.05$).

Epithelial barrier dysfunction in colon biopsies from *C. jejuni*-infected patients

Impedance spectroscopy measurements revealed a drop in epithelial resistance (R^{epi}) in *C. jejuni*-infected colon compared with healthy controls, whereas the subepithelial resistance (R^{sub})—which can cover and even hide overall epithelial resistance changes—remained unchanged (**Figure 2a**). Concomitantly, tracer flux measurements with fluorescein (332 Da) were performed and revealed an increase in permeability in *C. jejuni*-infected colon specimens when compared with healthy controls (**Figure 2b**). As additional marker we used FITC-dextran 4 kDa in parallel Ussing experiments that showed no alteration (**Figure 2c**). This indicates that the loss of the epithelial barrier function is rather due to changes in TJs and the number of apoptoses than to epithelial leaks as erosions (**Supplementary Figure S2**).

Epithelial apoptosis

As apoptotic lesions have significant impact on epithelial resistance and permeability of intermediate-sized molecules, we examined the induction of apoptosis in cross-sections of colon specimens by quantification of activated caspase-3 staining (**Figure 2d**). In the colon mucosa from *C. jejuni* patients, epithelial apoptotic ratio was increased from 0.5% in controls to 3% in *C. jejuni*-infected patients ($P<0.001$, $n=5$ each, **Figure 2e**). In the subepithelium, apoptotic ratio of lamina propria lymphocytes (LPL) appeared focally increased (reflected by high s.e.m.), but was unchanged to control values in the overall analysis (**Figure 2e**).

Molecular analysis of TJ proteins in human colon

Expression of several barrier-sealing TJ proteins was diminished in *C. jejuni*-infected epithelium (**Figure 3a**). Protein expression was quantified by the densitometric analysis and revealed a reduction of claudin-3, -4, -5, and -8 (**Figure 3a**). Occludin expression remained unchanged. Claudin-1 expression tended to be increased (not reaching statistical significance), but was redistributed in the enterocytes off the TJ anyway (see below). Claudin-2, a channel-forming claudin, also exhibited a tendency to be increased (**Figure 3b**), which just failed to reach statistical significance due to the high scattering of the values within the infected group (179 ± 41% vs. 103 ± 10% in controls, $P=0.11$, $n=5$).

In **Figure 3c**, mRNA expression analysis (RNA-Seq) of several TJ genes that were differentially expressed is shown (**Figure 3c**). The results were in agreement with the western blot data. Increased expression in *C. jejuni*-infected mucosae was found for claudin-1 and -2 mRNA (CLDN1, -2), whereas mRNA expression of barrier maintaining claudins, CLDN3, -4, and -8, was downregulated. The change in CLDN5, however, just failed to reach statistical significance in this analysis ($P=0.07$). Further claudins (CLDN7, -9, -11, -12, and -15) as well as tricellulin (MARVEL D2) were not altered and other claudins were not detected on mRNA level or have not been shown yet to be expressed on protein level in human colon.[16]

TJ protein distribution in confocal laser-scanning microscopy

The cellular distribution of TJ proteins was further characterized with confocal laser-scanning microscopy (CLSM). *Z*-axis scans (*xz* plane) showed claudins colocalized with zonula occludens protein-1 (ZO-1) within the TJ of controls, whereas immunostaining of infected patients revealed a redistribution of several claudins (**Figure 4**). In CLSM images, claudin-1 signals were retracted from TJ strands and appeared in the basolateral membrane and intracellular compartments (**Figure 4a**). Owing to the almost complete retraction from the TJ, the observed increase in claudin-1 mRNA expression levels becomes functionally dispensable (claudin-1 paradox). Also for claudin-5 and claudin-8, redistribution of the TJ was observed with a concomitant appearance of claudin aggregates near the basolateral membrane (**Figure 4b,c**). Moreover, the stained TJ pattern in the crypts of infected patients became discontinuous (**Figure 4b**). In summary, *C. jejuni* infection leads to an epithelial barrier dysfunction in human colon by

redistribution of claudin-1, -5, and -8, and furthermore by downregulation of claudin-3 and -4, as well as by induction of epithelial apoptosis, all of which can contribute to leak-flux diarrhea.

Differentially expressed genes in *C. jejuni*-infected mucosa and upstream regulator analysis

Further direct information from the acute infected human tissue was received by RNA-Seq that revealed 2,988 transcripts were downregulated and 2,410 upregulated (from four *C. jejuni*-infected patients and six controls, data are deposited in NCBI's Gene Expression Omnibus; GEO ID GSE88710). By means of these gene expression data, we determined the signaling pathways involved in this disease. For this purpose, we engaged Ingenuity pathway analysis (IPA). Here, an upstream regulator is ranked dependent upon its downstream target genes that are differentially regulated in the patients' mucosa. Upstream regulator means that the respective downstream pathways are activated or inhibited by expression regulation. From over 1,000 identified upstream regulators that had significantly altered downstream targets in *C. jejuni*-infected human mucosa, the most significant upstream regulator was lipopolysaccharide (LPS) with an overlap *P*-value of 3.22E − 66 and the highest activation *z*-score of 11.94. The second most significant hit was interferon-γ (IFNγ) signaling. The other top upstream regulators were also cytokines, six of which with predicted activation states are listed in **Table 2**. The activation *z*-score determines that an upstream transcription regulator has significantly more "activated" predictions ($z>0$) than "inhibited" predictions ($z<0$). Proinflammatory cytokines with barrier-affecting properties like IFNγ, tumor necrosis factor-α (TNFα), and interleukin-13 (IL-13) have been among the most significant pathways in this analysis (**Table 2**). A further proinflammatory cytokine pathway with high activation value was interleukin-1β (IL-1β), which showed an activation *z*-score of 8.57. On the other hand, a top hit with a prediction for inhibited pathways with equally high overlap *P*-value of 8.97E − 25 was the active vitamin calcitriol (*z*-score −6.25; with negative expression direction). The regulation pattern with inhibition of calcitriol-dependent pathways in the *C. jejuni*-infected mucosa led to the assumption that supplementation of calcitriol might counter-regulate the inhibition of downstream target genes. Further predicted regulator candidates are listed in the **Supplementary Information** (**Supplementary Table S2**). A more detailed explanation of regulators with a prediction of inhibited pathways is provided in the **Supplementary Information** in the respective paragraph of **Supplementary Table S2** "Signaling pathways in human colon biopsies".

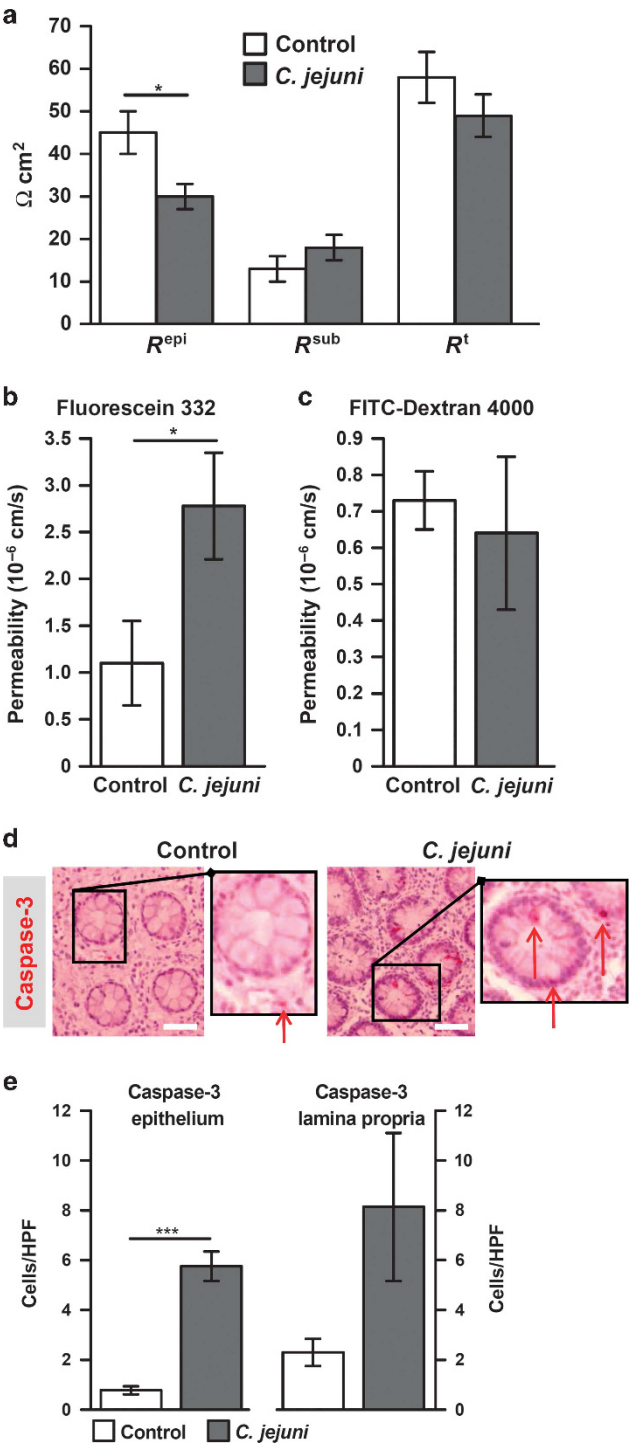

Figure 2 Epithelial leakage in the colon mucosa of *C. jejuni* patients. (**a**) Impedance spectroscopy delineated epithelial (R^{epi}) and subepithelial (R^{sub}) contributions to the overall transmural electrical resistance (R^{t}) in human colon biopsies. *$P<0.05$, Student's *t*-test, $n=6$ each. (**b**) Epithelial permeability in human colon mucosa for 332 Da fluorescein measured in Ussing chambers. *$P<0.05$, Student's *t*-test, $n=6$ *C. jejuni*-infected patients, $n=7$ controls. (**c**) Epithelial permeability for 4 kDa FITC-dextran, not significant, Student's *t*-test, $n=5$ *C. jejuni*-infected patients, $n=7$ controls. (**d**) Apoptosis induction. Representative microscopic images (×400 magnification) from activated caspase-3 (anti-cleaved caspase-3 antibody) immunohistochemistry with red-colored apoptosis induction in crypts of healthy and *C. jejuni*-infected colon (red arrows in crypt details indicate apoptotic events). White bars = 50 μm. (**e**) Quantification of apoptotic events. Single cells with cleaved caspase-3-positive signals were counted in high power fields (HPF), containing ~200 epithelial cells or lamina propria lymphocytes. ***$P<0.001$; Student's *t*-test, $n=5$ each group. Data represent mean ± s.e.m.

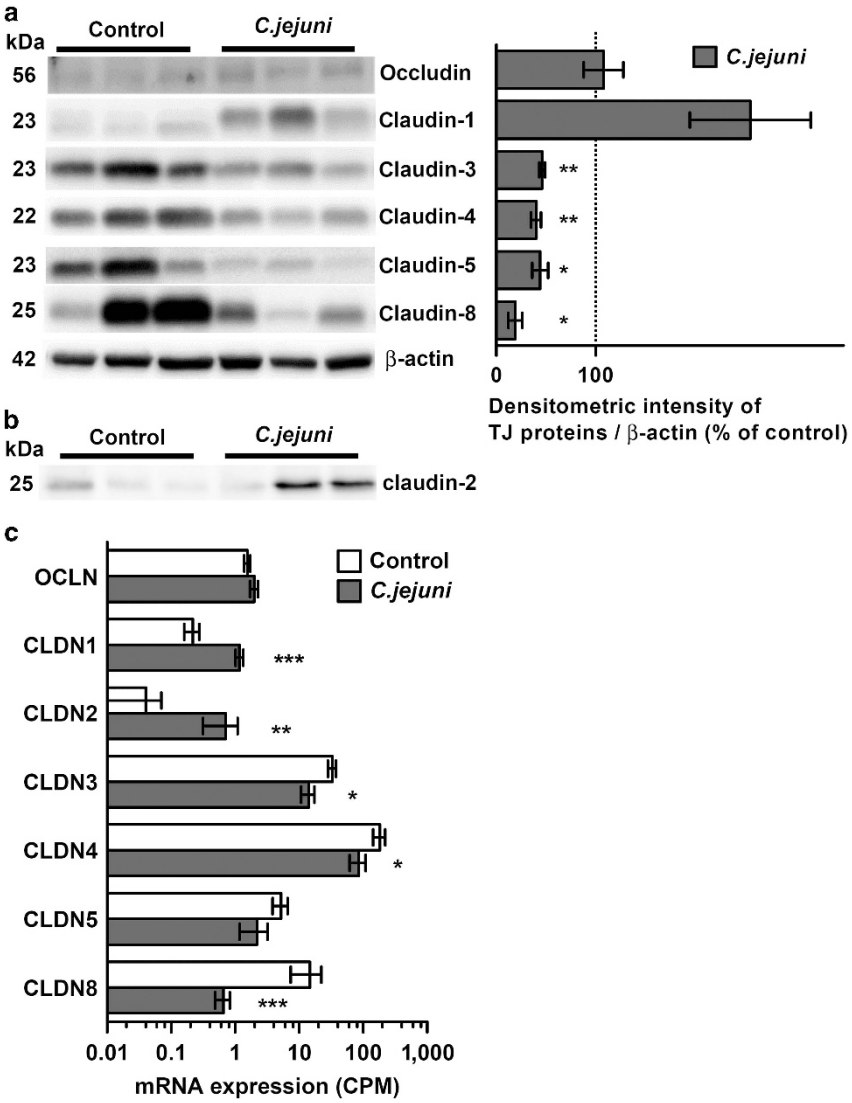

Figure 3 Tight junction (TJ) expression in campylobacteriosis. (**a**) Western blot and densitometry of TJ protein expression from human colon tissue. Expression of TJ proteins was normalized with β-actin level. $^{*}P<0.05$, $^{**}P<0.01$, Student's *t*-test, $n=5$ patients. (**b**) Western blot of channel-forming TJ protein claudin-2. (**c**) Differential gene expression analysis from RNA-Seq. mRNA expression of TJ genes (OCLN = occludin, CLDN = claudin) from fixed biopsies. Normalized expression is illustrated as logarithmic function and reflects counts per million (CPM) as calculated by edgeR with $^{*}P<0.05$, $^{**}P<0.01$, $^{***}P<0.001$ vs. controls, Fisher's exact test, $n=4$ *C. jejuni*-infected patients, $n=6$ controls. Data represent mean ± s.e.m.

Furthermore, additional information on canonical pathways is given in the (**Supplementary Table S3**).

Cytokine release in *C. jejuni*-infected colon

To confirm whether these identified cytokines which can functionally affect the epithelium were indeed released from the infected mucosae, we performed cytometric bead arrays in the supernatant of incubated mucosae from our patients. All predicted barrier-relevant proinflammatory cytokines (IFNγ, TNFα, IL-13, and IL-1β) were increased in *C. jejuni*-infected mucosa compared with healthy controls (**Figure 5**).

Experimental infection and cytokine incubation in HT-29/B6 cells *in vitro* mimics ENaC impairment and barrier dysfunction observed in the human host

We tested cytokines that are active in *C. jejuni* infection for their ability to induce similar changes as observed in our biopsies also in cell culture models, alone, or together with *C. jejuni*. In intestinal HT-29/B6-GR/MR cells[17] (human colon epithelial cell HT-29/B6-derived,[18] that exhibit ENaC activity[19]), the infection with *C. jejuni* led to a partial loss of ENaC activity after 48 h of infection (**Figure 6a**), and a decrease in TER (**Figure 6b**). By addition of a cytokine cocktail composed of IFNγ, TNFα, IL-13, and IL-1β to the basal medium of HT-29/B6-GR/MR cell monolayers, these effects were potentiated. Thus, co-incubation of *C. jejuni* and cytokines ((**Figure 6**) right columns) could qualitatively and quantitatively mimic the effects on ENaC and barrier function seen in the patients' biopsies.

Epithelial barrier regulation by experimental infection in co-cultures of immune cells and epithelial cells

As GM-CSF (granulocyte macrophage colony-stimulating factor, CSF2) as an inductor of M1-macrophages is an

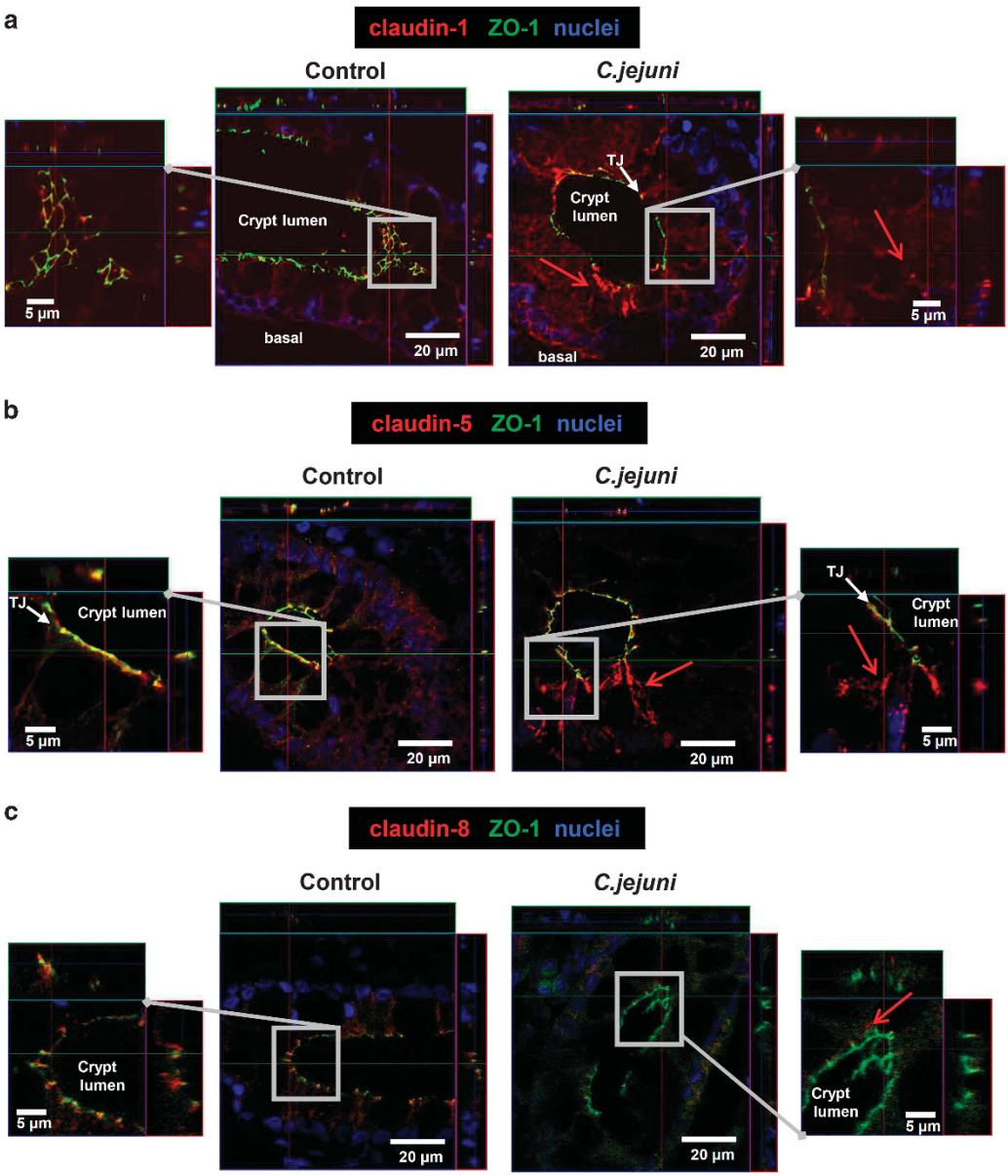

Figure 4 Tight junction (TJ) protein distribution in campylobacteriosis. Representative confocal laser-scanning micrographs of human colon crypts from immunostaining against Zonula occludens protein-1 (ZO-1, green) and claudins (red) with (**a**) claudin-1, (**b**) claudin-5, (**c**) claudin-8. Nuclei are colored blue by 4′-6-diamidino-2-phenylindole dihydrochloride (DAPI) staining. Colocalization of two TJ proteins appears as yellow merge. White arrows indicate the TJ. Red arrows indicate claudin redistribution. A full color version of this figure is available at the *Mucosal Immunology* journal online.

upstream regulator with high impact in *C. jejuni* enteritis (**Table 2**), we conducted co-culture experiments with M1-macrophages and HT-29/B6 epithelial cells as described previously.[20] As reported earlier in several cell culture models (Caco2, T84) TER was not affected during *C. jejuni* invasion and remains stable during invasion up to 24 h post infection.[10] The same is true in HT-29/B6 cells. However, when co-cultured with M1-macrophages in the basal compartment, TER drops already at 24 h p.i. (**Figure 7**), when HT-29/B6 cell monolayers were infected by *C. jejuni* with the same multiplicity of infection (MOI) of 100. Thus, the secondary effect of macrophage activation by *C. jejuni* has a more significant impact on epithelial barrier function than the bacteria alone, most likely via cytokine release.

Inhibitory effect of vitamin D on *C. jejuni*-induced cytotoxicity

To test the efficiency of the predicted regimen calcitriol (active vitamin D) against *C. jejuni* pathology in human colon mucosa, we conducted a cytotoxicity assay (WST-assay) for *C. jejuni* in HT-29/B6 cells supplemented with 10–200 nM of calcitriol vs. controls (**Figure 8**). By prolonged incubation in microaerobic atmosphere and a higher infectious dose, the cytotoxic effect of *C. jejuni* became evident. With calcitriol supplementation, the

Table 2 Upstream regulator analysis

Upstream regulator	Overlap *p*-value	Activation *z*-score	Number of genes that have expression direction consistent with activation of the cytokine
LPS	3.22E – 66	11.94	343 (of 501 affected downstream targets)
IFNγ	3.95E – 44	9.62	253 (of 370 affected downstream targets)
CSF2	2.58E – 42	10.15	144 (of 182 affected downstream targets)
TNFα	3.23E – 41	9.00	279 (of 462 affected downstream targets)
IL-6	1.18E – 38	7.25	134 (of 236 affected downstream targets)
IL-13	1.39E – 30	2.12	87 (of 145 affected downstream targets)
IL1β	1.54E – 24	8.57	165 (of 236 affected downstream targets)

Abbreviations: CSF2, granulocyte macrophage colony-stimulating factor; IFNγ, interferon-gamma; IL, interleukin; LPS, lipopolysaccharide; TNFα, tumor necrosis factor-alpha. Top upstream regulators, lipopolysaccharide (LPS) and proinflammatory cytokines with highly significant activation of their downstream targets in colon specimens from patients with campylobacteriosis (4 patients vs. 6 healthy controls). Column 1; gene name of the upstream regulator. Column 2; *P*-value of the overlap of the downstream target gene set and the pathway gene set. Column 3; Activation *z*-score. Column 4; number of genes with expression changes. The complete list of genes differentially expressed in patients with *C. jejuni* and controls, which are downstream targets of the upstream regulator is provided in the (**Supplementary Table S2**). For target gene names, see supplementary spreadsheet online (**Supplementary Table S2 online**). The overlap *P*-value measures whether there is a statistically significant overlap between the data set genes and the genes that are regulated by an upstream transcriptional regulator. It is calculated using Fisher's exact test, and significance is generally attributed to *P*-values <0.01. A statistical approach defines a quantity (*z*-score) that determines whether an upstream transcription regulator has significantly more "activated" predictions than "inhibited" predictions ($z>0$) or vice versa ($z<0$).

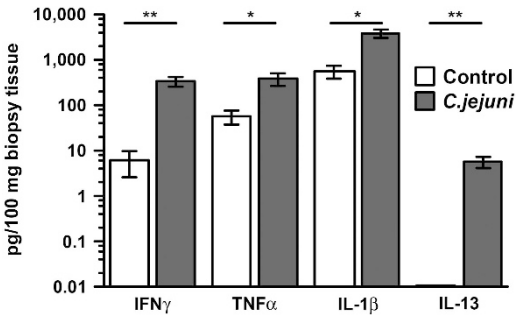

Figure 5 Mucosal cytokine release in *Campylobacter jejuni* infection. Cytokine production of colonic biopsies from healthy subjects and patients with *C. jejuni* enteritis of interferon-γ (IFNγ), tumor necrosis factor-α (TNFα), interleukin-13 (IL-13), and interleukin-1β (IL-1β). $^*P<0.05$, $^{**}P<0.01$, Student's *t*-test with Holm–Bonferroni adjustment for multiple comparisons, $n=5$ each group. Data represent mean ± s.e.m.

cytotoxicity could be inhibited (>50 nM) or completely abolished (200 nM) in this experimental setup. Furthermore, we gained first evidence that calcitriol could exhibit protective/therapeutic action in *C. jejuni* infection also on barrier function, as we measured a partial recovery in TER from *C. jejuni*-infected HT-29/B6 cell monolayers supplemented with 200 nM calcitriol. When HT-29/B6 monolayers were infected shortly after confluence and incubated in ambient air for 3 days, TER decreased from 1,448 ± 34 to 146 ± 43 Ω cm^2 after *C. jejuni* vs. 479 ± 105 Ω cm^2 with vitamin D and *C. jejuni* ($P<0.05$, $n=6$, Student's *t*-test).

DISCUSSION

C. jejuni infection is the most common cause of zoonotic gastroenteritis with frequent chronic manifestations. Nevertheless, *C. jejuni*-induced pathologies are far from being understood.[6,7] For the first time, we present direct data from the infected human mucosa by functional and parallel molecular analysis in human campylobacteriosis. Thus, a novel view on the *Campylobacter* infection is depicted which even allows us to predict remedies for evaluation in clinical studies.

Impaired active ion transport in the *Campylobacter*-infected colon

The first main finding of this study is the disturbed epithelial sodium transport by downregulation of β- and γ-ENaC subunits. We could show by measurements of the J_{Na} that in acute campylobacteriosis Na^+ absorption in the colon is impaired. Hence, we found for the first time evidence for Na^+ malabsorption as diarrheal mechanism in this disease. Similar pathology of disturbed ENaC function could be shown, e.g., for lymphocytic colitis.[21] As regulatory influence from these studies, the involvement of the Th1 cytokines TNFα and IL-1β in the downregulation of ENaC activity is well documented and has been shown to be due to expression regulation of β- and γ-ENaC subunits from the gene[22] and/or MAP kinase-dependent inactivation.[21] Only recently, also the inhibitory influence of IL-13 on ENaC was enlightened in cell and mouse models.[19] In case of the *Campylobacter*-induced ENaC disturbance, we found that already the bacteria per se can impair ENaC activity *in vitro*, an effect that is intensified by the cytokines IFNγ, TNFα, IL-13, and IL-1β that are induced in the acute phase of infection and released from LPL after invasion of the bacteria into deeper mucosal layers (cryptitis). Similar results were also obtained from a mouse infection model of salmonellosis, in which ENaC dysregulation as well as CFTR and DRA downregulation resulted in malabsorptive diarrhea.[23] In our patients, the mRNA counts of CFTR and DRA were also reduced. On the one hand, this is in accordance with our reduced maximal transport capacity after stimulation of CFTR-dependent electrogenic Cl^- secretion. The reduction in basal short-circuit current excludes a cholera-like toxin-mediated secretory component of the *Campylobacter* diarrhea. On the other hand, the reduction in DRA mRNA level in our patients points to a disturbance also of the second important Na^+

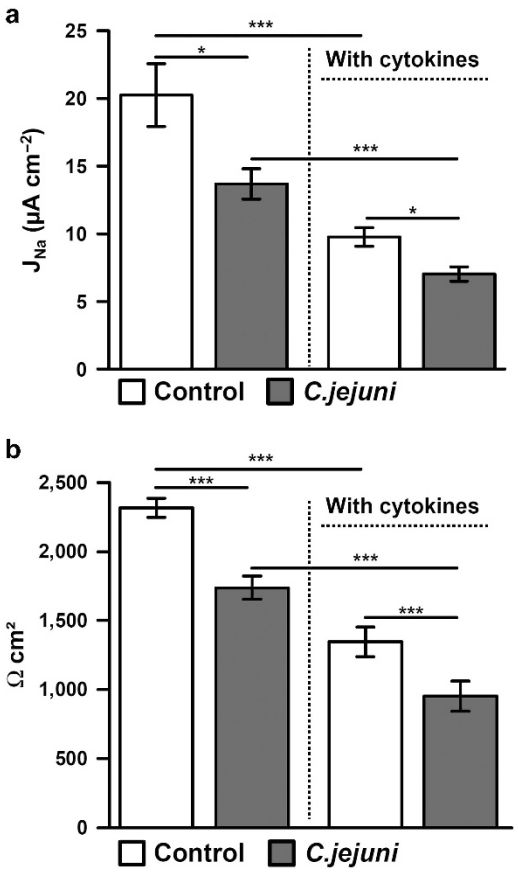

Figure 6 Experimental infection of HT-29/B6-GR/MR cell monolayers. (**a**) Electrogenic sodium transport (J_{Na}) in untreated control monolayers, *C. jejuni*-infected or cytokine cocktail-treated epithelial cell monolayers, or co-treatment. To induce ENaC activity, cells were pre-stimulated for 5 days with 5×10^{-8} M dexamethasone, 2×10^{-3} M sodium-butyrate, 3×10^{-9} M aldosterone as described before.[19] *C. jejuni* infection dose; multiplicity of infection (MOI) 100, infection duration; 48 h, addition of low-dose cytokine cocktail, consisting of recombinant human interferon-γ (10 U ml^{-1}), tumor necrosis factor-α (10 U ml^{-1}), interleukin-13 (10 ng ml^{-1}), and interleukin-1β (10 ng ml^{-1}), cytokine incubation; 24 h. I_{SC} was measured in Ussing chambers before and after ENaC inhibition with amiloride (10^{-4} M), which was added to the mucosal compartment. The drop in I_{SC} was attributed to the ENaC-dependent Na^+ flux (J_{Na}). $n = 6$ cell monolayers each group. (**b**) Transepithelial electrical resistance (Ω cm^2) of the respective cell monolayers and conditions above, measured at the same incubation endpoints and after addition of amiloride. $n = 12$. $^*P < 0.05$, $^{**}P < 0.01$, $^{***}P < 0.001$, Student's *t*-test with Holm–Bonferroni adjustment for multiple comparisons. Data represent mean ± s.e.m.

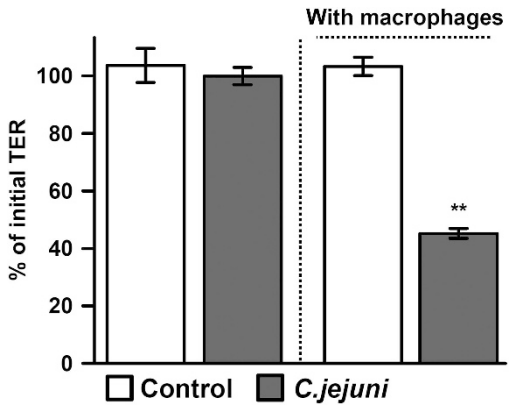

Figure 7 Epithelial cell—immune cell co-culture after 24 h of incubation with either *Campylobacter jejuni* or M1-macrophages or both. Transepithelial electrical resistance of HT-29/B6 cell monolayers, apically infected with *C. jejuni* (MOI 100) drops earlier by activation of macrophages. Experimental setting; GM-CSF (50 U ml^{-1}) was used for M1-macrophage differentiation. M1-macrophages in the basal compartment were co-cultured with HT-29/B6 monolayers.[20] $n = 4$, $^{**}P < 0.01$, Student's *t*-test with Holm–Bonferroni adjustment. Data represent mean ± s.e.m.

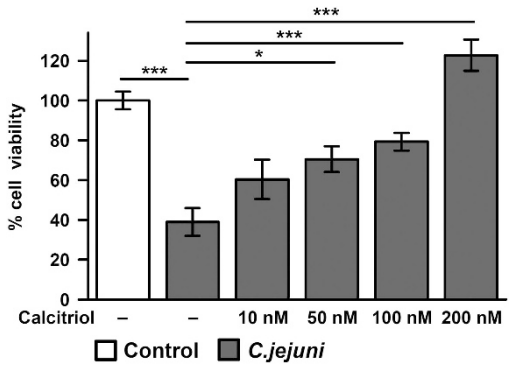

Figure 8 Inhibition experiments with active vitamin D. Fort-eight hours of incubation with *Campylobacter jejuni*, MOI 500 in microaerobic atmosphere revealed a loss of epithelial HT-29/B6 cell viability in WST cytotoxicity test. Inhibitory concentrations of 50–200 nM calcitriol could block the *C. jejuni*-induced epithelial cell loss. $n = 8$, $^*P < 0.05$, $^{***}P < 0.001$, Student's *t*-test with Holm–Bonferroni adjustment.

absorptive mechanism of the colon, the electroneutral NaCl absorption.[24] Taken together, reduced transport of Na^+ by disturbed absorptive ion transporters (ENaC, DRA) are important pathomechanisms of the *Campylobacter* colitis.

Campylobacter-induced barrier dysfunction

As second important result of our study, we could illuminate the epithelial barrier defect with increased paracellular permeability towards small macromolecules in *C. jejuni*-infected human mucosa by TJ dysregulation and as already proposed before for *C. jejuni* by an induction of apoptosis in the epithelium. Both defects result in diarrhea along a leak-flux mechanism. This pathomechanism by downregulation of claudin-3, -4, and -8 via expression regulation from the gene and change in subcellular localization of claudin-1, -5, and -8 by redistribution of the TJ could be shown here for the first time as main contributor for the *C. jejuni*-induced pathogenicity. Similar results on claudin-5 were obtained before for experimental *Arcobacter butzleri* or *Campylobacter concisus* infection in HT-29/B6 cells, two closely related pathogens.[25,26] The induction of claudin-1 and -2 after proinflammatory activation could be shown before.[27–29] The paradox induction of claudin-1 in *C. jejuni*-infected mucosae (higher claudin-1 expression with lower resistance due to claudin-1 redistribution off the TJ) can be triggered by proinflammatory cytokines via NFκB.[27] In inflammatory situations, as e.g., ulcerative colitis, an upregulation of the channel-forming claudin-2 was observed, which is considered to cause diarrhea but which has also been discussed

to represent a protective mechanism to rinse off noxious agents from the mucosa.[28,29] Also, it has been shown before that claudin-2 upregulation can occur via PI3-kinase signaling, induced by TNFα and IFNγ, or via STAT6 activation by IL-13.[16,28,30] In case of the *C. jejuni* infection, several barrier-forming claudins were downregulated or subcellularly redistributed reflecting a severe breakdown of the epithelial barrier. However, the mucosal inflammatory response is crucial for this TJ effects in campylobacteriosis as indicated by the *C. jejuni*-infected co-culture experiments with epithelial cells and macrophages.

Apoptosis induction and lesions

As apoptosis has been reported to have an important role in the *C. jejuni* pathology, we quantified this effect also in our human biopsy specimens. In recent *in vitro* studies, we found induction of epithelial apoptosis between 1 and 5% to have significant effects on TER and molecule marker fluxes.,[2526,31] Both, induction of apoptosis by the apoptosis inductor campthotecin and by *Campylobacter concisus* share the result of a decrease in TER and an increase in fluorescein flux with a cut-off in molecule flux size with unchanged 4 kDa dextran permeabilities.[26,32] The flux measurements from the mucosae of our patients revealed the same tracer flux pattern with increased fluorescein permeability (332 Da) and a cut-off at 4 kDa in campylobacteriosis.

Also in acute *Giardia lamblia* or norovirus infection,[33,34] other intestinal infections with diarrhea as the main symptom, a combined disturbance of barrier function and ion transport have been detected, pointing to intestinal barrier dysfunction being especially relevant during impaired Na^+ absorption. This was one of the reasons for looking into the acute infection in human mucosae and to quantify the functional defects. There we found an epithelial apoptotic ratio of 3% in *C. jejuni*-infected tissue, which would according to cell model data cause a decrease in TER by about 25%.[32]

Invasion of *C. jejuni* could be observed in CLSM pictures, but a colocalization of bacteria and apoptotic events was not observed, again supporting the 4 kDa cut-off of apoptotic barrier defects. However, gross lesions (erosions) could be identified in infected crypts, and here a colocalization with the invaded bacteria was seen (**Supplementary Figure S2**). Thus, transmigration of bacteria across the epithelium can happen through epithelial leaks and subsequently provoke immune response in the subepithelium, whereas small luminal antigens will cross the impaired epithelial barrier via the paracellular pathway due to TJ defects and apoptotic events in the epithelium during campylobacteriosis. Subsequent barrier defects are accelerated after bacterial transmigration as indicated by the experimental infection, in which bacterial exposure is much more effective from the basolateral (for simulation of bacterial subvasion) than from the mucosal side of cell monolayers.[11,25,26]

Transcriptome and upstream signaling analysis in campylobacteriosis

The bioinformatics' predictions calculated from RNA-Seq in conjunction with the IPA upstream regulator analysis revealed proinflammatory cytokine pathways to be involved in human campylobacteriosis, which is the third main finding of this study. The cytokines with most significant overlap *P*-values or highest activation scores were revealed to be IFNγ, TNFα, IL-13, and IL-1β, all of which were also known to have significant impact on epithelial transport and barrier function.[31,35,36]

Moreover, GM-CSF (CSF2) and interleukin-6 (IL-6) were found in our IPA upstream regulator analysis of acute campylobacteriosis. Although GM-CSF, in contrast to IL-6,[37] has not been shown to be directly barrier-relevant, it represents an important differentiation factor for M1-macrophages and can indirectly regulate barrier function.

Within the data record of regulators revealed by IPA not only biologically involved key players of pathway activation were found, but also potential effectors were predicted that would inhibit pathways when theoretically applied to the inflammatory situation (for a more detailed explanation see the **Supplementary Information** paragraph "Signaling pathways in human colon biopsies").

The finding of LPS and peptidoglycan to be important in the IPA ranking with activating pathways emphasizes the relevance of the intestinal barrier for restriction of luminal antigen influx.[38] Thus, a quick recovery from intestinal leakage after administration of protective substances like quercetin, which is barrier-protective[39] and a predicted counter-regulator (**Supplementary Table S2**), is a promising regimen for barrier restoration and subsequent protection from the *Campylobacter*-induced sequelae.

Among the predicted drugs, which may influence disease outcome, are immunosuppressants or inhibitors of the PI3-pathway like Ly294002 or sirolimus (rapamycin), the latter of which was shown to promote recovery from *C. jejuni* infection in a mouse colitis model.[40] The most feasible candidate for future studies in *C. jejuni* infection is calcitriol (vitamin D), which showed the most significant influence on downstream targets in the category of drugs and may serve as clinical option for recovery from *C. jejuni* enteritis (**Supplementary Table S2**). Active vitamin D modulates proinflammatory and anti-inflammatory cytokines and could improve the Th1/Th2 balance in immune cells,[41] which could result in an accelerated clearance of *C. jejuni* from the mucosa. Furthermore, this vitamin shows anti-apoptotic action in keratinocytes.[42] In our present study, we observed protection by calcitriol against cell death and barrier dysfunction also in colon HT-29/B6 enterocytes during *C. jejuni* exposure. These inhibition experiments point to altered cell proliferation and TJ protein expression and the effects seem to depend on the differentiation state of the cells as well as the signaling in vitamin D receptor downstream targets. Vitamin D status has been found to be relevant also for chronic inflammatory conditions as ulcerative colitis.[43] Hence, in further studies a protective action of vitamin D supplementation during or after the *C. jejuni* infection should be elaborated for prevention of sequelae developing from the leaky gut. Also, the efficacy of its protective action in multimodal regimens (e.g., vitamin D, quercetin, and zinc) is worth to be investigated in further studies. Additional

information from IPA for canonical intracellular pathways show significant immune cell-specific pathways like TREM1 (Triggering receptor expressed on myeloid cells-1) and epithelium-specific pathways like aldosterone signaling and tight/gap junction signaling (see **Supplementary Table S3** "Canonical pathways in *Campylobacter jejuni*-infected human colon mucosa.xls").

In conclusion, (i) sodium malabsorption and epithelial leak-flux as a result of barrier dysfunction in the colon are responsible for diarrhea in campylobacteriosis. (ii) Release of proinflammatory cytokines such as IFNγ, TNFα, IL-1β, and IL-13 substantially aggravated the *C. jejuni*-mediated epithelial defects. (iii) Insights into pathomechanisms and signaling pathways of *C. jejuni* enteritis, together with bioinformatics' predictions, are inevitable for the development of therapeutic interventions and supplementation regimens. (iv) Regimens that ameliorate the intestinal barrier dysfunction could protect against unwanted antigen influx through the leaky gut and prevent *C. jejuni*-associated complications like reactive arthritis and post-infectious IBS.

METHODS

Ethics statement. For the use of human material this study adhered to the Declaration of Helsinki. The study was approved by the Ethics Committee of the Charité under the approval number EA4/123/09 and written informed consent was obtained from all patients 24 hours prior to the intervention.

Study design and clinical characteristics of *C. jejuni*-infected patients. Patients underwent routine colonoscopy due to acute diarrhea or for preventive examination, and biopsies were taken from the sigmoid colon 30 cm *ab ano*. For electrophysiological measurements (impedance spectroscopy), colonic biopsies were mounted into Ussing chambers. The time between removal of biopsies from the colon and mounting into Ussing chambers was 20–30 min. The remaining biopsies were immediately fixed in liquid nitrogen and stored ($-80\,^{\circ}C$) for molecular biological approaches, as immunofluorescence staining for CLSM or western blotting, or RNA-sequencing (RNA-Seq) (**Supplementary Figure S1**). The diagnosis of *C. jejuni* infection was confirmed subsequently by stool culture, and the patient's data could be allocated to the respective study group. In the control group, inflammatory parameters were normal. *C. jejuni*-positive patients were in the acute phase of infection between 3 to 7 days after the first symptoms had occurred and showed increased C-reactive protein (CRP) levels between 20 and 150 $mg\,l^{-1}$ and increased blood leukocyte counts between $11.7 \times 10^9 l^{-1}$ and $16.7 \times 10^9 l^{-1}$. The reported symptoms were mainly watery diarrhea with abdominal cramps and stool frequencies of 10–20 times in 24 h. The patients group for impedance spectroscopy (**Supplementary Table S1**) consists of four females and two males with a mean age of 37 years (range 19–53), the control group consists of three males and three females with a mean age of 43 years (range 24–64) and underwent colonoscopy for the prevention of colon cancer.

Electrophysiological investigations. The biopsies were mounted in miniaturized Ussing chambers (0.049 cm^2 area) and analyzed performing one-path impedance spectroscopy and unidirectional flux measurements of 0.1 mM fluorescein (332 Da; Sigma-Aldrich, St. Louis, MO, USA) or 0.3 mM dialyzed fluorescein isothiocyanate (FITC)-dextran-4000 (4 kDa; TdB Consultancy, Uppsala, Sweden) under voltage-clamp conditions as described previously.[38]

Impedance spectroscopy. The total transepithelial resistance (R^t) of the intestinal barrier consists of two components, epithelial (R^{epi}) and subepithelial resistance (R^{sub}), which can be distinguished as previously described.[44] A detailed description is provided in the **Supplementary Information**.

Short-circuit current (I_{SC}). I_{SC} of human colonic biopsies was recorded in parallel. At the end of each experiment, addition of theophylline (10^{-2} M) and prostaglandin E_2 (PGE_2, 10^{-6} M), followed by carbachol (10^{-4} M) determined the secretory response of the epithelium. Inhibition of Cl^- secretion was measured after addition of bumetanide (10^{-5} M).

Electrogenic Na^+ transport. In parallel, human biopsy specimens, mounted in Ussing chambers, were stimulated with aldosterone (3×10^{-9} M). Eight hours after addition of aldosterone, the ENaC blocker amiloride (10^{-4} M) was added to the mucosal compartment and the resulting drop in I_{SC} was attributed to ENaC-dependent Na^+ flux as described previously.[21]

Protein analysis by immunohistochemistry, western blotting, and CLSM. Tissues were fixed in 2% paraformaldehyde (3 h) for immunostaining and microscopic analysis or immediately stored in liquid nitrogen for protein expression analysis by western blotting. Immunohistochemistry (cleaved caspase-3 antibody, Cell Signaling Technology, Danvers, MA, USA, Cat. no. #9661) and densitometric analysis from western blots for TJ analysis as well as CLSM was performed as described previously.[16,38] A detailed description with the complete list of antibody numbers is provided in the **Supplementary Information**.

Next-generation sequencing and RNA-Seq expression analysis

RNA isolation from human colon biopsies. RNA was extracted with the Trizol (Invitrogen, Carlsbad, CA, USA) reagent according to the manufacturer's protocol including a DNase digestion step with the RNase-free DNase set from Qiagen (Hilden, Germany). The integrity was assessed using the Agilent BioAnalyzer 2100 (Ratingen, Germany) Technology.

Library preparation of RNAs. cDNA library preparation and sequencing was performed by Illumina's RNA-Seq prep kit following the manufacturer's instructions. The purified DNA was quantified and diluted to 10 nM for cluster generation and sequencing on an Illumina HiSeq 2500 (Eindhoven, The Netherlands).

Primary sequencing data analysis. Fastq files were obtained after demultiplexing using Illuminas CASAVA v1.8.2 pipeline with default parameters. Secondary analysis: Reads were mapped against the human genome GRCh37/hg19 using STAR v2.4.2a with double pass alignment.[45] First mapping was obtained using Ensembl v73 coordinates as a framework, whereas the second mapping added splice sites, which were found in the first pass.

RNA-Seq expression analysis. Gene-read coverages were obtained using STAR aligners "–quantMode GeneCounts" option. All subsequent analyses were done using the edgeR package in R. Expression changes were calculated as log2 ratios of the read counts per transcript for two investigated conditions, and ratios were normalized using the weighted-trimmed mean of M-values (TMM). Counts per million values (CPM) were normalized with TMM correction over all mapped sequences. *P*-values were corrected for multiple testing according to Benjamini Hochberg to match the false discovery rate (FDR) and a cut-off of $P<0.05$ (5% FDR) was chosen. The mucosal architecture of the biopsies used for RNA-Seq did not differ with respect to the proportion of epithelial cells and lymphocytes or submucosal thickening. Overall, 14,467 of 60,669 genes (24%) were expressed in either infected or control tissues, reflecting a good coverage. The median absolute deviation (MAD) was slightly higher within the control samples as compared to the infected group (median (across all expressed genes) control: 1.1, infected: 0.98). This points to higher "natural" inter-individual variability in the control group and more similar expression profiles in the infected group, which suggests synchronization of gene expression by inflammation. Upstream regulators and canonical pathways were identified with the Ingenuity Pathway Analysis software (Qiagen Silicon Valley, Redwood City, CA, USA).

Data availability. RNA-Seq data are deposited in NCBI's Gene Expression Omnibus and can be accessed as GSE88710. The authors declare that all data supporting the findings of this study are available within the article and its supplement. Other raw data are available from the corresponding author upon request.

Mucosal cytokine induction. Cytokine release of the infected mucosa was measured by cytometric bead array (CBA) after an incubation of the live mucosa in LPL-medium with high oxygen (80% O_2) and slight shaking. Biopsies were cultured for 48 h, as described previously[46] and cytokines produced *in situ* were quantified in the supernatants with CBA (Becton Dickinson, Heidelberg, Germany) according to manufacturer's protocol.

Cell culture and experimental infection. Human colon cell models HT-29/B6 and HT-29/B6-GR/MR (with stable-transfected glucocorticoid receptor (GR) and mineralocorticoid receptor (MR)) were cultured in RPMI cell culture medium (RPMI 1640, Sigma-Aldrich) as described previously.[17,18,19] *Campylobacter jejuni* 81-176 reference strain was precultured in respective cell culture medium and applied to the apical side of the monolayers with an MOI 100 or 500. Recombinant human cytokines (PeproTech, Rocky Hill, CT, USA) were applied to the basal compartment of cell monolayers.
Cytotoxicity. Cell viability was tested in 96-wells with confluent HT-29/B6 cells (75,000 cells per well) at day 8 after seeding. Cell Counting Kit-8 (WST-assay) was performed according to manufacturer's instructions (Dojindo Laboratories, Munich, Germany).
Co-culture. Monocytes from PBMC preparation were stimulated for one week with GM-CSF (PeproTech, Rocky Hill, CT) for M1 differentiation. M1-macrophages in the basal compartment were co-cultured with HT-29/B6 monolayers grown to confluency on filter inserts in parallel as described previously.[20]

Statistics. Data are expressed as mean ± s.e.m. Statistical analysis was performed using two-tailed Student's *t*-test with Holm–Bonferroni adjustment for multiple comparisons. NGS data sets were compared by Fisher's exact test as described above. $P < 0.05$ was considered to be statistically significant.

SUPPLEMENTARY MATERIAL is linked to the online version of the paper at http://www.nature.com/mi

ACKNOWLEDGMENTS

In-Fah Maria Lee and Diana Bösel are gratefully acknowledged for their technical support. Funding for this study was supported by the Deutsche Forschungsgemeinschaft (DFG Schu559/11) to J.D.S; the Volkswagen Foundation (Lichtenberg program) to M.R.S. and the German Federal Ministry of Education and Research (BMBF) PAC-CAMPY consortium (IP8) to R.B. and J.D.S.

AUTHOR CONTRIBUTIONS

Conceived and designed the experiments: R.B., J.D.S., C.Ba., T.S. Performed the experiments: R.B., S.M.K., A.F., C.Ba., V.M. Acquisition of biopsy material from endoscopy: C.Bo., C.Ba., T.S. Analyzed the data: R.B., S.M.K., V.M., M.K., M.R.S., S.J., A.F., C.Ba. Important intellectual support: M.R.S., M.F., T.S., B.S. Contributed reagents/materials/analysis tools: J.D.S., S.M.K., V.M., S.J., N.A.H., C.Bo., M.F., M.R.S., M.K. Wrote the paper: R.B. Critical revision and study supervision: N.A.H., C.Ba., B.S., J.D.S. The final version of the manuscript was revised and approved by all authors.

DISCLOSURE

The authors declared no conflict of interest.

ETHICS APPROVAL

For the use of human material this study adhered to the Declaration of Helsinki, and ethics approval for research was obtained from The Ethics Committee of the Charité—Universitätsmedizin Berlin (Approval Number EA4/123/09). All patients who participated in the investigation signed written informed consent forms 24 hours prior to the intervention. Children were not included in the study.

DISCLAIMER

The funders had no role in study design, data collection, analysis, decision to publish, or preparation of the manuscript.

REFERENCES

1. Blaser, M.J. *et al.* Experimental *Campylobacter jejuni* infection of adult mice. *Infect. Immun.* **39**, 908–916 (1983).
2. Russell, R.G. *et al.* Experimental *Campylobacter jejuni* infection in *Macaca nemestrina*. *Infect. Immun.* **57**, 1438–1444 (1989).
3. Fox, J.G. *et al.* Gastroenteritis in NF-kappaB-deficient mice is produced with wild-type *Camplyobacter jejuni* but not with *C. jejuni* lacking cytolethal distending toxin despite persistent colonization with both strains. *Infect. Immun.* **72**, 1116–1125 (2004).
4. Hickey, T.E. *et al.* Intracellular survival of *Campylobacter jejuni* in human monocytic cells and induction of apoptotic death by cytholethal distending toxin. *Infect. Immun.* **73**, 5194–5197 (2005).
5. Elmi, A. *et al. Campylobacter jejuni* outer membrane vesicles play an important role in bacterial interactions with human intestinal epithelial cells. *Infect. Immun.* **80**, 4089–4098 (2012).
6. Black, R.E. *et al.* Experimental *Campylobacter jejuni* infection in humans. *J. Infect. Dis.* **157**, 472–479 (1988).
7. Spiller, R.C. *et al.* Increased rectal mucosal enteroendocrine cells, T lymphocytes, and increased gut permeability following acute *Campylobacter enteritis* and in post-dysenteric irritable bowel syndrome. *Gut* **47**, 804–811 (2000).
8. van Spreeuwel, J.P. *et al. Campylobacter colitis*: histological immunohistochemical and ultrastructural findings. *Gut* **26**, 945–951 (1985).
9. Boehm, M. *et al.* Rapid paracellular transmigration of *Campylobacter jejuni* across polarized epithelial cells without affecting TER: role of proteolytic-active HtrA cleaving E-cadherin but not fibronectin. *Gut Pathog* **4**, 3 (2012).
10. Backert, S. *et al.* Transmigration route of *Campylobacter jejuni* across polarized intestinal epithelial cells: paracellular, transcellular or both?. *Cell Commun. Signal.* **11**, 72 (2013).
11. Chen, M.L. *et al.* Disruption of tight junctions and induction of proinflammatory cytokine responses in colonic epithelial cells by *Campylobacter jejuni*. *Infect. Immun.* **74**, 6581–6589 (2006).
12. Lamb-Rosteski, J.M. *et al.* Epidermal growth factor inhibits *Campylobacter jejuni*-induced claudin-4 disruption, loss of epithelial barrier function, and *Escherichia coli* translocation. *Infect. Immun.* **76**, 3390–3398 (2008).
13. Rees, L.E. *et al.* Campylobacter and IFNgamma interact to cause a rapid loss of epithelial barrier integrity. *Inflamm. Bowel Dis.* **14**, 303–309 (2008).
14. Soler, A.P. *et al.* Activation of NF-kappaB is necessary for the restoration of the barrier function of an epithelium undergoing TNF-alpha-induced apoptosis. *Eur. J. Cell Biol.* **78**, 56–66 (1999).
15. Negoro, S. *et al. Campylobacter jejuni* infection suppressed Cl^- secretion induced by CFTR activation in T-84 cells. *J. Infect. Chemother.* **20**, 682–688 (2014).
16. Zeissig, S. *et al.* Changes in expression and distribution of claudin 2, 5 and 8 lead to discontinuous tight junctions and barrier dysfunction in active Crohn's disease. *Gut* **56**, 61–72 (2007).
17. Bergann, T. *et al.* Glucocorticoid receptor is indispensable for physiological responses to aldosterone in epithelial Na^+ channel induction via the mineralocorticoid receptor in a human colonic cell line. *Eur. J. Cell Biol.* **90**, 432–439 (2011).
18. Kreusel, K.M. *et al.* Cl^- secretion in epithelial monolayers of mucus-forming human colon cells (HT-29/B6). *Am. J. Physiol.* **261**, C574–C582 (1991).
19. Dames, P. *et al.* Interleukin-13 affects the epithelial sodium channel in the intestine by coordinated modulation of STAT6 and p38 MAPK activity. *J. Physiol.* **593**, 5269–5282 (2015).
20. Lissner, D. *et al.* Monocyte and M1 macrophage-induced barrier defect contributes to chronic intestinal inflammation in IBD. *Inflamm. Bowel Dis.* **21**, 1297–1305 (2015).

21. Barmeyer, C. *et al.* ENaC dysregulation through activation of MEK1/2 contributes to impaired Na^+ absorption in lymphocytic colitis. *Inflamm. Bowel Dis.* **22**, 539–547 (2016).
22. Barmeyer, C. *et al.* IL-1beta and TNFalpha regulate sodium absorption in rat distal colon. *Biochem. Biophys. Res. Commun.* **317**, 500–507 (2004).
23. Marchelletta, R.R. *et al.* Altered expression and localization of ion transporters contribute to diarrhea in mice with *Salmonella*-induced enteritis. *Gastroenterology* **145**, 1358–1368 (2013).
24. Bachmann, O. & Seidler, U. News from the end of the gut—how the highly segmental pattern of colonic HCO^- transport relates to absorptive function and mucosal integrity. *Biol. Pharm. Bull.* **34**, 794–802 (2011).
25. Bücker, R. *et al. Arcobacter butzleri* induces barrier dysfunction in intestinal HT-29/B6 cells. *J. Infect. Dis.* **200**, 756–764 (2009).
26. Nielsen, H.L. *et al.* Oral and fecal *Campylobacter concisus* strains perturb barrier function by apoptosis induction in HT-29/B6 intestinal epithelial cells. *PLoS ONE* **6**, e23858 (2011).
27. Amasheh, M. *et al.* TNFalpha-induced and berberine-antagonized tight junction barrier impairment via tyrosine kinase, Akt and NFkappaB signaling. *J. Cell. Sci.* **123**, 4145–4155 (2010).
28. Weber, C.R. *et al.* Claudin-1 and claudin-2 expression is elevated in inflammatory bowel disease and may contribute to early neoplastic transformation. *Lab. Invest.* **88**, 1110–1120 (2008).
29. Poritz, L.S. *et al.* Increase in the tight junction protein claudin-1 in intestinal inflammation. *Dig. Dis. Sci.* **56**, 2802–2809 (2011).
30. Mankertz, J. *et al.* TNFalpha up-regulates claudin-2 expression in epithelial HT-29/B6 cells via phosphatidylinositol-3-kinase signaling. *Cell. Tissue Res.* **336**, 67–77 (2009).
31. Bojarski, C. *et al.* Apoptosis and intestinal barrier function. *Ann. N.Y. Acad. Sci.* **915**, 270–274 (2000).
32. Bojarski, C. *et al.* Permeability of human HT-29/B6 colonic epithelium as a function of apoptosis. *J. Physiol.* **535**, 541–552 (2001).
33. Troeger, H. *et al.* Effect of chronic *Giardia lamblia* infection on epithelial transport and barrier function in human duodenum. *Gut* **56**, 328–335 (2007).
34. Troeger, H. *et al.* Structural and functional changes of the duodenum in human norovirus infection. *Gut* **58**, 1070–1077 (2009).
35. Weber, C.R. *et al.* Epithelial myosin light chain kinase activation induces mucosal interleukin-13 expression to alter tight junction ion selectivity. *J. Biol. Chem.* **285**, 12037–12046 (2010).
36. Heller, F. *et al.* Epithelial apoptosis is a prominent feature of the epithelial barrier disturbance in intestinal inflammation: effect of pro-inflammatory interleukin-13 on epithelial cell function. *Mucosal Immunol.* **1**, S58–S61 (2008).
37. Suzuki, T. *et al.* Interleukin-6 (IL-6) regulates claudin-2 expression and tight junction permeability in intestinal epithelium. *J. Biol. Chem.* **286**, 31263–31271 (2011).
38. Bücker, R. *et al.* α-Haemolysin of *Escherichia coli* in IBD: a potentiator of inflammatory activity in the colon. *Gut* **63**, 1893–1901 (2014).
39. Amasheh, M. *et al.* Quercetin enhances epithelial barrier function and increases claudin-4 expression in Caco-2 cells. *J. Nutr.* **138**, 1067–1073 (2008).
40. Sun, X. *et al. Campylobacter jejuni* induces colitis through activation of mammalian target of rapamycin signaling. *Gastroenterology* **142**, 86–95 (2012).
41. Daniel, C. *et al.* Immune modulatory treatment of trinitrobenzene sulfonic acid colitis with calcitriol is associated with a change of a T helper (Th) 1/Th17 to a Th2 and regulatory T cell profile. *J. Pharmacol. Exp. Ther.* **324**, 23–33 (2008).
42. De Haes, P. *et al.* Molecular pathways involved in the anti-apoptotic effect of 1,25-dihydroxyvitamin D3 in primary human keratinocytes. *J. Cell Biochem.* **93**, 951–967 (2004).
43. Stio, M. *et al.* Vitamin D regulates the tight-junction protein expression in active ulcerative colitis. *Scand. J. Gastroenterol.* **20**, 1–7 (2016).
44. Bürgel, N. *et al.* Mechanisms of diarrhea in collagenous colitis. *Gastroenterology* **123**, 433–443 (2002).
45. Dobin, A. *et al.* STAR: ultrafast universal RNA-seq aligner. *Bioinformatics* 29, 15–21 (2013).
46. Schneider, T. *et al.* Increased immunoglobulin G production by short term cultured duodenal biopsy samples from HIV infected patients. *Gut* **42**, 357–361 (1998).